Recrystallization Following Hot-Working of a High-Strength Low-Alloy (HSLA) Steel and a 304 Stainless Steel at the Temperature of Deformation

T. L. CAPELETTI, L. A. JACKMAN, AND W. J. CHILDS

The recovery and recrystallization behavior of two commercial quality steels, a Cb(Nb) strengthened high-strength low-alloy (HSLA) steel and a 304 stainless steel, was studied following hot-working. Specimens were deformed in tension at a constant head velocity of 2 in./s to reductions-in-area of 30 to 50 pct at temperatures in the austenite range from 1600° to 1900°F. The subsequent annealing behavior was observed at the temperature of deformation. Decreasing recrystallization rates with decreasing temperature and/or deformation were observed. It is suggested that CbC precipitation occurred during annealing of the HSLA steel and accounted for an arrest in the softening behavior. For the 304 stainless steel it is concluded that dynamic recrystallization took place during deformation, that thermal microtwinning was an active recovery mechanism during annealing, and that there was a preference for grain boundaries as nucleation sites for recrystallized grains. These conclusions regarding the annealing behavior of 304 stainless steel were supported by metallographic analysis of specimens water quenched from the temperature of deformation.

DURING the plastic deformation of metals there are changes in substructure and microstructure which are well documented and which depend upon many variables.[1,2] One of the primary variables is the temperature at which the metal is deformed, giving rise to two broad divisions termed hot- and cold-working. The basic aspects of these two forms of deformation have been defined by many other investigators.[1,3-7] Independent of whether the metal is deformed by hot- or cold-working, when held at elevated temperatures, following deformation, the metal will undergo structural changes tending to return it to the undeformed condition.

The two basic softening processes are recovery[1,5-9] and recrystallization.[1,5,7,10-13] Byrne[1] has summarized the mechanisms of recovery as a function of the annealing temperature. He indicated the importance of microtwinning as a possible recovery mode at intermediate to high temperatures. This will be discussed in more detail in a later portion of this presentation. Several workers have also summarized the effects of different variables on the rate of recrystallization.[1,2,6,11,12,14-16] Of particular interest is the general effect of decreasing recrystallization rates with decreasing annealing temperature and/or deformation. Another aspect of importance to this study is the effect of second-phase particles.[17] This depends not only upon the size and dispersion of the particles but also upon whether they are present prior to working or form during annealing following working.[2] In addition, several investigators have indicated the preference for grain boundaries as nucleation sites for recrystallized grains,[6,7,18,19] particularly following hot-working.

As the temperature of deformation increases, the softening mechanisms become increasingly important. The behavior of the metal during deformation is then determined by the relative rates of strain hardening and softening. There are two main theories concerning the softening mechanism operating during hot-working. One theory maintains that the only possible mechanism is dynamic recovery,[4,9] while the other theory maintains that dynamic recovery occurs at small strains, but dynamic recrystallization takes place at large strains, if recovery is inhibited.[20-22] These two theories and the evidence involved in their formulation have been summarized and reviewed very eloquently by Stüwe,[5] Tegart,[23] and Jonas *et al.*[6] Briefly, the operating mechanism depends upon the ease with which recovery can take place, which depends primarily upon the stacking-fault energy.

Until recently, most studies of annealing following deformation have involved cold-working.[2,14,18,24-33] Some studies have involved hot-working,[16,20,34-36] but all of these have used various room temperature measurements (*e.g.* hardness measurements and metallographic analysis) which are obscured by the allotropic phase transformation which takes place on cooling in low-alloy steels. Consequently, it is desirable to have a method of following the annealing process at the temperature of annealing. With this in mind Wilbur *et al.*[37] developed a technique whereby the softening behavior of the metal could be observed following hot-work, at the temperature of deformation. A form of this technique has been applied to a high-strength low-alloy steel by Cordea and Hook.[38] Their results are interesting, but did not include very short annealing times due to their method of controlling the deformation. The extent of deformation was controlled by an adjustable cylindrical sleeve positioned to limit the

T. L. CAPELETTI, formerly with Rensselaer Polytechnic Institute, Troy, New York, is now Associate Senior Research Metallurgist with General Motors Research Laboratories, Warren, Mich. L. A. JACKMAN is Assistant Professor, Rensselaer Polytechnic Institute. W. J. CHILDS, formerly Professor, Rensselaer Polytechnic Institute, is now Technical Representative, Duffers Associates, Troy, N. Y. This paper is based upon a thesis submitted by T. L. CAPELETTI in partial fulfillment of the requirements of the degree of Doctor of Philosophy at Rensselaer Polytechnic Institute.

Manuscript submitted May 21, 1971.

Table I. Chemical Compositions of Materials Studied (Pct)

	C	Mn	Si	Mo	Al	Cb
HSLA 304	0.11	0.84	0.29	0.31	0.03	0.032
	0.053	1.64	0.016	0.053	–	–
	B	N	P	S	Cr	Si
HSLA 304	0.003	0.006	0.018	0.025	–	–
	–	–	0.026	0.016	18.42	8.69

travel of the load cylinder. Readjustment of the sleeve took 5 to 7 s and that established the minimum delay time. This restriction was avoided in the present investigation where the technique of Wilber *et al.* was applied to two commercial quality steels at elevated temperatures in the austenite range.

EXPERIMENTAL DETAILS

A) Materials and Specimen Geometry

The compositions of the materials used in this investigation are given in Table I. They consisted of a Cb strengthened high-strength low-alloy (HSLA) steel and a 304 stainless steel. Both were commercial quality materials and were tested in the as-received condition in the form of $\frac{1}{4}$ in. diam round bars. These bars were cut to lengths of $4\frac{1}{2}$ in. (HSLA) and $4\frac{3}{4}$ in. (304) and the ends were threaded. The heated gage lengths were 1.0 in. (HSLA) and $1\frac{1}{2}$ in. (304) with deformation gage lengths of approximately $\frac{1}{4}$ in. (HSLA) and $\frac{1}{3}$ in. (304). The specimens were resistance heated, however, making it difficult to determine the deformation gage length with any real accuracy due to the presence of an axial thermal gradient. The specimens were deformed to reductions-in-area of 30 to 50 pct, at temperatures of 1600° to 1900°F, at a constant head velocity of 2 in./s in an argon atmosphere.

B) Apparatus

The primary testing apparatus was the "Gleeble", a device specifically designed for the study of elevated temperature mechanical properties and the effects of various thermomechanical cycles on those properties.[39] Basically, the apparatus employs a resistance-heated specimen, with water-cooled copper jaws. Thermal and mechanical cycles are programmed on an electronic function generator to duplicate any desired thermomechanical treatment. The loading is pneumatically actuated and hydraulically controlled to maintain a constant head velocity. The raw data is recorded automatically on a direct print visicorder.

C) Experimental Technique

The technique consists of thermally treating the material according to a predetermined program, deforming in tension at the hot-working temperature to a desired RA, holding at temperature for various delay times, and then deforming to fracture. A schematic diagram of the load-time curve for this sequence of events is given in Fig. 1. The first curve represents the initial deformation; it is followed by unloading and holding for the delay time Δt. The second curve represents the final deformation to fracture. As a measure

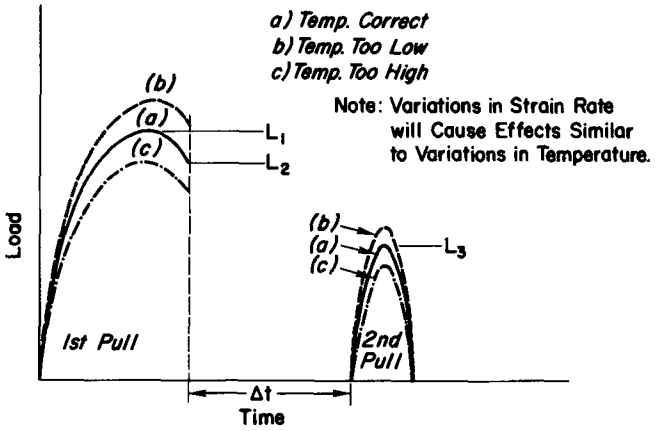

Fig. 1—Load-time schematic for measuring recrystallization.

of the softening which takes place during the delay time (Δt), the quantity $L_3 - L_2$ is plotted as a function of (log Δt), where

Δt = Delay time (sec)

L_2 = Load at unload on the first deformation (pound force)

L_3 = Peak load on the second deformation (pound force)

If there are no structural changes during a given delay time then $L_3 = L_2$ and $L_3 - L_2 = 0$. As softening occurs L_3 decreases and $L_3 - L_2$ becomes increasingly more negative. When the structural change is essentially completed, $L_3 - L_2$ levels off at some maximum softening value.

D) Metallography

In order to correlate microstructural changes with the load-softening data for the 304 stainless steel, specimens were subjected to the same thermal-mechanical cycles but water quenched to room temperature instead of being deformed to fracture. A special quenching device was constructed to produce an essentially cylindrical quenching volume in order to conform as closely as possible to the specimen geometry. After quenching, these samples were mounted and mechanically polished by standard procedures. They were then electropolished in a perchloric and ethanol solution and etched electrolytically at 10 v in 10 pct oxalic acid to reveal the structure.

E) Thermal-Mechanical Cycles

The specific thermal-mechanical cycles used with each material tested are given in Table II. The thermal cycle for the HSLA steel was designed to austenitize the material and also to put the columbium in solution. This required a peak temperature of 2300°F[20,40,41] which is somewhat higher than that which would otherwise be employed to austenitize columbium free steels. The thermal cycle for the 304 stainless was designed to homogenize the material prior to deformation.

F) Measures of Structural Change

In addition to the load change ($L_3 - L_2$) used by Wilber *et al.*, another parameter which should be indica-

Table II. Thermal-Mechanical Cycles

1) HSLA Steel
Heated to 2300°F in 5 s
Held at 2300°F for 15 s
Cooled to Test Temperature in 5 s
Held at Test Temperature for 5 s
Loaded in Tension at 2 in./s to 30 ± 4 pct or 50 ± 5 pct RA
Held for various delay times
Reloaded to fracture

2) 304 Stainless Steel
Heated to 2100°F in 10 s
Held at 2100°F for 20 s
Cooled to test temperature in 10 s
Held at test temperature for 10 s
Loaded in tension at 2 in /s to 35 ± 4 pct or 50 ± 5 pct RA
Held for various delay times
Reloaded to fracture or water quenched to R.T.

tive of structural change during annealing is ductility. Although ductility, as measured by the reduction-in-area at fracture, may be complicated by other processes, such as precipitation, it should lend support to the load softening data in some cases. The ductility parameter used in this investigation was the RA at fracture, based upon the area which remained after the first deformation. Briefly, the RA after the first deformation was monitored using the elongation data, as printed out on the visicorder trace, and the RA at fracture was measured with a low-power microscope equipped with a filar eye-piece. The ductility parameter was then reduced to

$$RA_3 = \left(\frac{RA_2 - RA_1}{100 - RA_1}\right)(100)$$

where

RA_1 = Reduction-in-area after the first deformation based on the original cross-sectional area.

RA_2 = Total reduction-in-area at fracture based on on the original cross-sectional area as measured with the microscope.

RA_3 = Reduction-in-area at fracture based on the area which remained after the first deformation.

The parameter RA_3 was then plotted as a function of (log Δt).

RESULTS AND DISCUSSION

A) HSLA Steel

The results of the annealing study on the HSLA steel are given in Figs. 2 and 3. In Fig. 2 the load-softening curves [$(L_3 - L_2)$ vs (log Δt)] are given for the softening following 50 pct RA at 1650° and 1900°F. The curves do not display a simple sigmoidal form, but contain offsets during the softening process. The first offset occurs at short delay times and relatively small values of softening. This was observed by Wilber *et al.*[37] and was explained on the basis of recovery mechanisms. This stage of the softening behavior appears to be relatively temperature independent, at least at the temperatures involved in this investigation. Following the initial offset, the softening proceeds by a thermally-activated mechanism as indicated by the

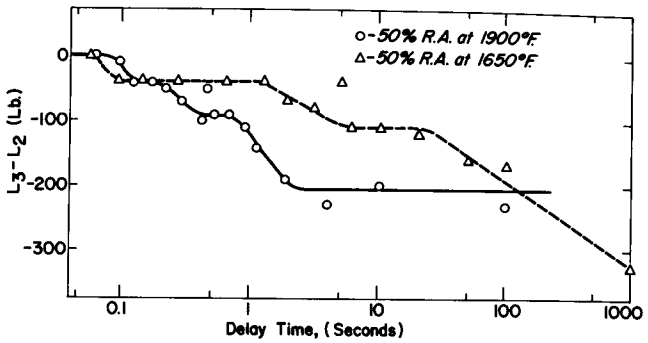

Fig. 2—Recrystallization of HSLA steel deformed 50 pct at 1650° and 1900°F—load softening.

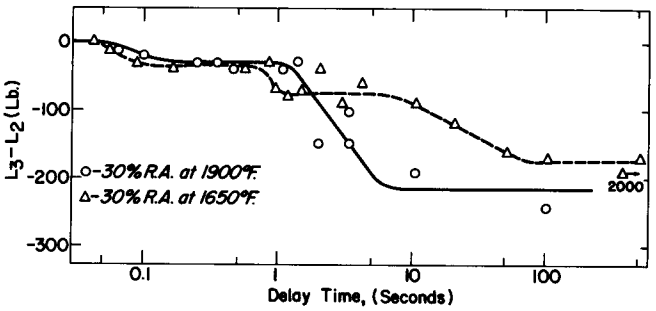

Fig. 3—Recrystallization of HSLA steel deformed 30 pct at 1650° and 1900°F—load softening.

shift in softening to longer delay times with decrease in temperature. During this portion of the softening another offset occurs at intermediate delay times and softening values. This offset appears to be different from the first offset by virtue of the fact that it is very temperature dependent and occurs during the thermally-activated portion of the softening. This data suggests that a precipitate (presumably CbC) forms during annealing and acts to restrict the migration of the recrystallizing grain boundaries, giving rise to an interruption in the softening process. Extraction replica studies of longitudinal sections of the specimens used to obtain these data were inconclusive. Some precipitates were observed which seemed to coarsen with time, but no real correlation with the data was observed. There was some indication that 15 s at 2300°F was not sufficient to completely dissolve the Cb(CN). This could account for some of the scatter in the results.

In Fig. 3, the load-softening curves are given for 30 pct RA at 1650° and 1900°F. These curves, in general, display the same behavior as those for 50 pct deformation. Comparison of the load-softening curves in Figs. 2 and 3 for 30 and 50 pct deformation at 1900°F illustrates the shift to longer delay times as the deformation decreases, an expected result.

The theoretical basis for second phase particles inhibiting grain boundary migration was first proposed by Zener as discussed by Smith.[17] Basically, the second-phase particles inhibit grain boundary migration by surface tension effects, when they lie within the boundary. In order to be effective, the surface tension must resist the driving force causing the migration. It is generally believed that second-phase particles can inhibit migration during grain growth, due to the low driving force for growth, but not during primary

recrystallization when the driving force for migration is high. However, there has been a great deal of recent evidence that precipitation, during annealing after cold-working, can indeed inhibit boundary migration during recrystallization.[2,13,24,25,27,29-31,33] Similarly, there is evidence of inhibition by precipitation following hot-work.[20,34,36,42] Many of these investigations show migrating boundaries clearly "scalloped" at their intersections with second-phase particles.

The results of Farrell *et al.*[33] are particularly interesting. They observed that small gas bubbles can substantially raise the recrystallization temperature of cold-worked high-purity tungsten. Gas bubble formation on dislocations and subgrain boundaries was seen using electron microscopy. This caused scalloping of the subgrain boundaries and advancing recrystallized grain boundaries. Recrystallization was quite sluggish and occurred substantially only after the bubbles coarsened to a few relatively large bubbles. The difference in kinetics of gas bubble formation and solid-phase precipitate formation notwithstanding, it appears that the explanation of Farrell *et al.* can be applied to the results obtained in this investigation on the HSLA steel. Specifically, the model proposed is that CbC or Cb(CN) precipitates on migrating subboundaries and recrystallized grain boundaries inhibiting the boundary migration and thus the softening. Only after the precipitates coarsen to a larger, more ineffective morphology does recrystallization proceed to completion. This is consistent with the mechanism of recrystallization by subgrain growth or coalescence.

As previously indicated, there is some indication that the Cb(CN) may not have been completely put into solution by the austenitizing treatment. It also appears that the precipitates are not very stable at 1900°F. Indeed, the short length of the offset following 50 pct deformation at 1900°F is probably due to resolution rather than coarsening. Precipitation and resolution of carbides during annealing following hot-working has been observed using X-ray analysis by Gulyayev and Shigarev.[34] Further, 30 pct deformation at 1900°F does not appear to be sufficient to consistently give rise to the precipitation effect observed in the other data. The net result is significant scatter in the data, which makes the existence of well-defined offsets questionable. Neglecting the offsets, however, the data still indicates a reduced rate of softening immediately following the recovery stage, followed by an increased

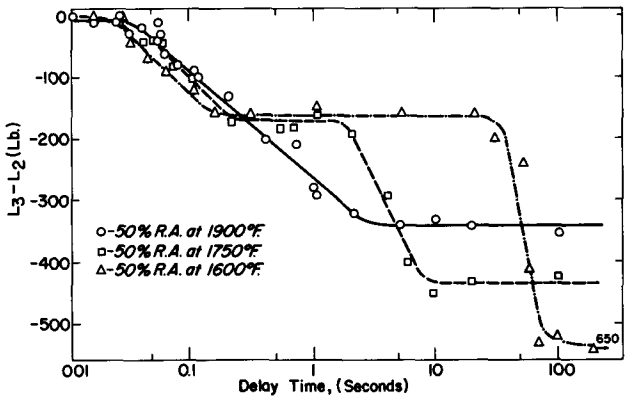

Fig. 4—Recrystallization of 304 stainless steel deformed 50 pct at 1600°, 1750°, and 1900°F—load softening.

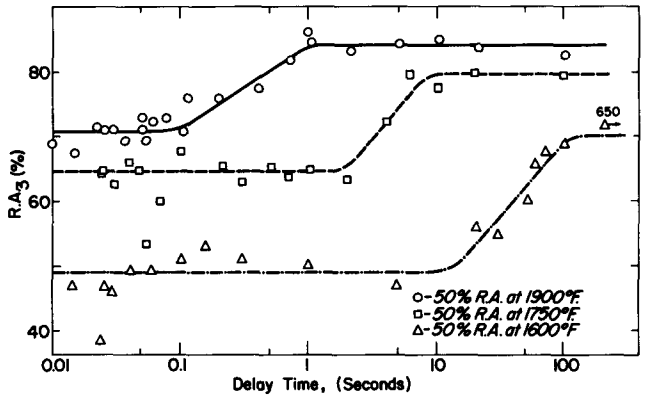

Fig. 5—Recrystallization of 304 stainless steel deformed 50 pct at 1600°, 1750°, and 1900°F—ductility change.

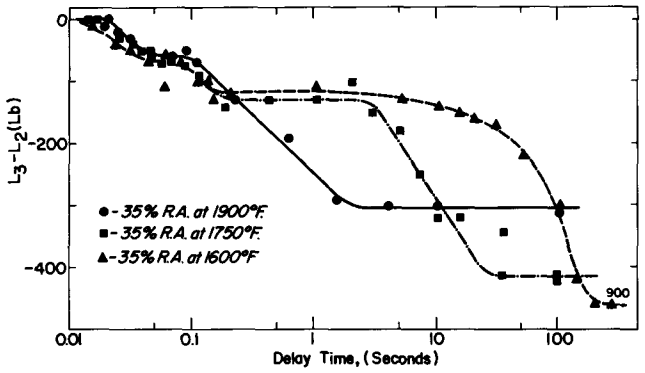

Fig. 6—Recrystallization of 304 stainless steel deformed 35 pct at 1600°, 1750°, and 1900°F—load softening.

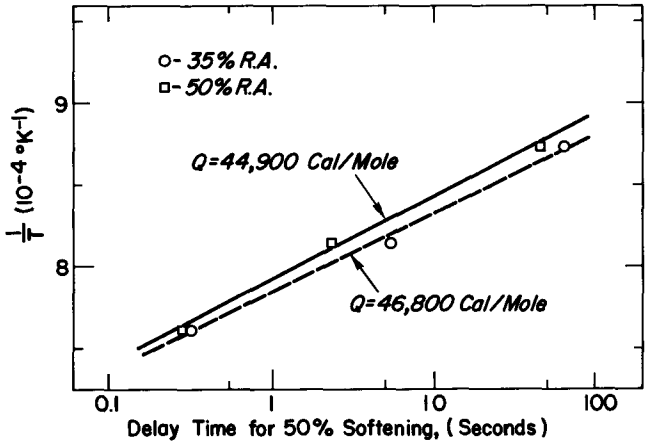

Fig. 7—Recrystallization of 304 stainless steel—Arrhenius plot.

rate preceding complete softening. The precipitation model remains valid, even for this interpretation of the data.

In comparison with the results of Wilber *et al.*,[37] these data exhibited the same general trends. Although Wilber *et al.*[37] did not observe any offsets which could be interpreted as being due to precipitate formation, their results displayed the same general behavior as that observed in the present investigation. It is interesting to note that the data of Cordea and Hook[38] displayed a reduced rate of softening for short delay times, followed by an increased rate preceding complete softening, particularly for the vanadium treated steel. In view of the discussion in the preceding para-

graph, this behavior is similar to that observed in the present investigation and may be due to precipitation during annealing.

B) 304 Stainless Steel

1) LOAD-SOFTENING AND DUCTILITY CHANGE

The load-softening and ductility change data obtained for the 304 stainless steel are given in Figs. 4 through 7. The general features of this data are the same as that for the HSLA steel. There is, in general, a recovery stage which is relatively temperature independent followed by a temperature-dependent softening stage during which the major portion of the softening takes place. The data also displays the shift to longer delay times with decreasing temperature or deformation.

In Fig. 4 the load-softening data is given for 50 pct

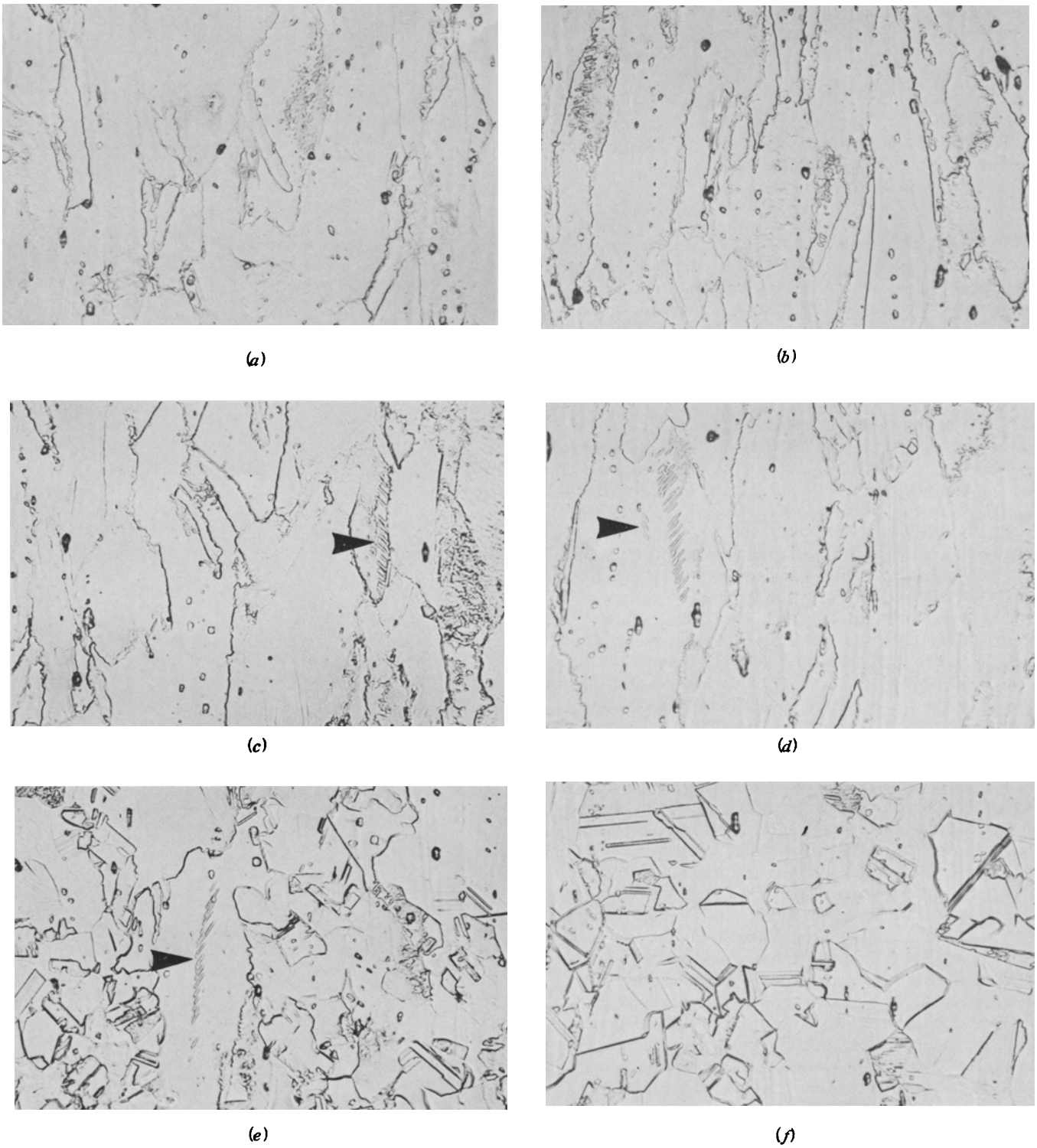

(a) (b) (c) (d) (e) (f)

Fig. 8—Microstructural changes during annealing of 304 stainless steel following 50 pct deformation at 1750°F. Magnification 567.5 times. (a) Δt = 0.007 s; (b) Δt = 0.33 s; (c) Δt = 0.073 s; (d) Δt = 0.140 s; (e) Δt = 2.5 s; (f) Δt = 15 s.

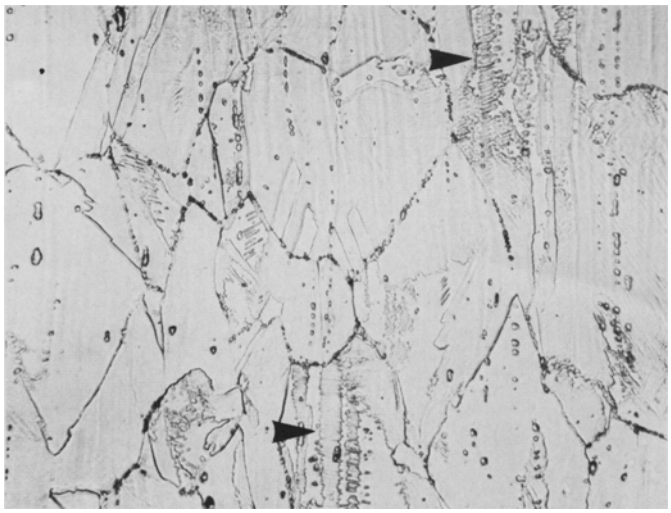

Fig. 9—Dense microtwin formations following 35 pct deformation at 1600°F. Magnification 445 times.

RA at 1600°, 1750°, and 1900°F. Offsets are again observed in the curves at intermediate delay times and softening values. These offsets are different from those observed for the HSLA steel, however, in that the softening prior to the offset is relatively temperature independent, while the softening after the offset is the more typically expected thermally-activated behavior. Scatter in the data has generally obscured the existence of the recovery offsets. The offset was observed for deformation at 1750°F, but it is difficult to separate from the data points for the other curves. The scatter precludes the observation of both offsets at 1900°F. In Fig. 5 the ductility change is given for 50 pct RA at 1600°, 1750°, and 1900°F. The data of Fig. 5 correlates directly with the load-softening data in Fig. 4. A substantial increase in ductility at fracture can be correlated only with the thermally-activated portion of the softening. There is no indication of a change in ductility associated with the recovery stage.

In Fig. 6 the load-softening data is given for 35 pct RA at 1600°, 1750°, and 1900°F. The curves display the same features as those for 50 pct deformation. Also, the ductility change data again correlates directly with the load-softening behavior, not shown here for the sake of brevity.

These observations indicate that a relatively temperature-independent recovery mode operates to produce a substantial amount of softening with little or no increase in ductility. One possible recovery mode which could account for this behavior is thermal microtwinning in the substructure.[1] This is consistent with the low stacking-fault energy. Burke and Turnbull[11] have described the mechanism of annealing twin formation and growth. They suggested that stacking faults produced during deformation provide ready-made nuclei for such twins. The model proposed to account for the behavior observed in this investigation is that the deformed material undergoes a recovery stage which consists of two portions, dislocation rearrangement and annihilation and thermal microtwin formation. These mechanisms act to relieve those areas of highest strain energy. Once the high energy areas are exhausted the softening ceases until thermally activated recrystallization occurs.

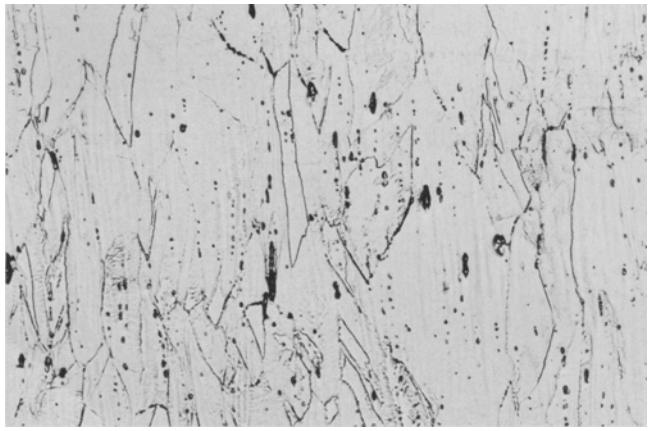

(a)

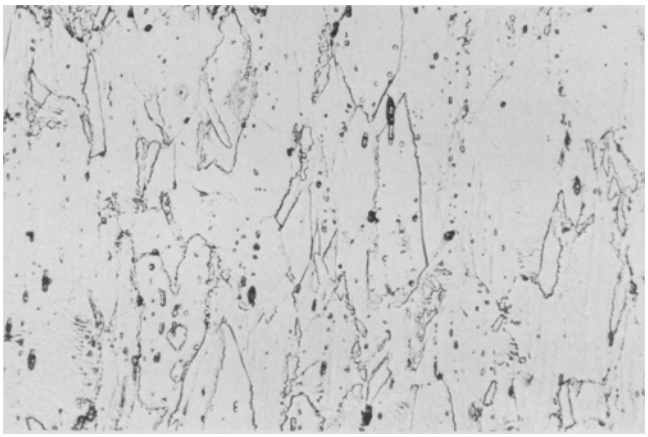

(b)

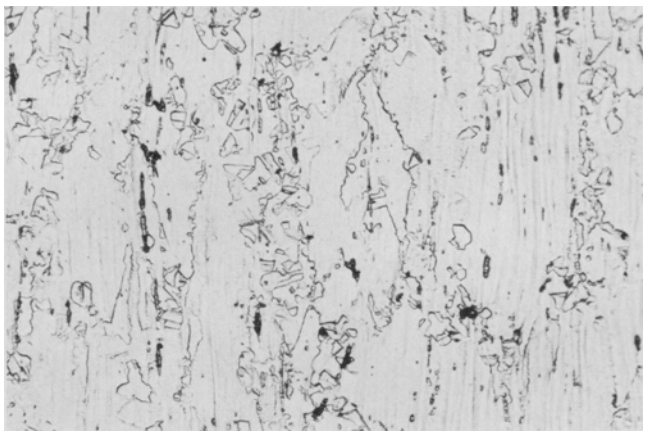

(c)

Fig. 10—Microstructure of 304 stainless steel as deformed 50 pct. Magnification 283 times. (*a*) 1600°F; (*b*) 1750°F; (*c*) 1900°F.

The temperature and deformation dependence of the rate of softening is summarized in Fig. 7. It is assumed that the softening obeys an Arrhenius relationship of the form

$$t_{0.5} = A \exp (Q/RT)$$

where

$t_{0.5}$ = Delay time for 50 pct softening

Q = Apparent activation energy

T = Absolute temperature at which $t_{0.5}$ is measured

and R has its usual meaning. From the slopes of the linear relationships in Fig. 7 the apparent activation energies are found to be

Q = 46,800 cal/mole for 35 pct deformation

and

Q = 44,900 cal/mole for 50 pct deformation

It must be emphasized, however, that these activation energies are only apparent values and cannot be related to any fundamental processes. This is due to the fact that no attempt has been made to separate the recovery stage from the recrystallization stage of softening, nor has any attempt been made to separate nucleation from growth. The values do indicate the dependence of softening on temperature, however, and also the decrease in activation energy with increase in deformation.

2) OPTICAL METALLOGRAPHY

Fig. 8 shows a typical series of micrographs displaying the changes in microstructure with increasing

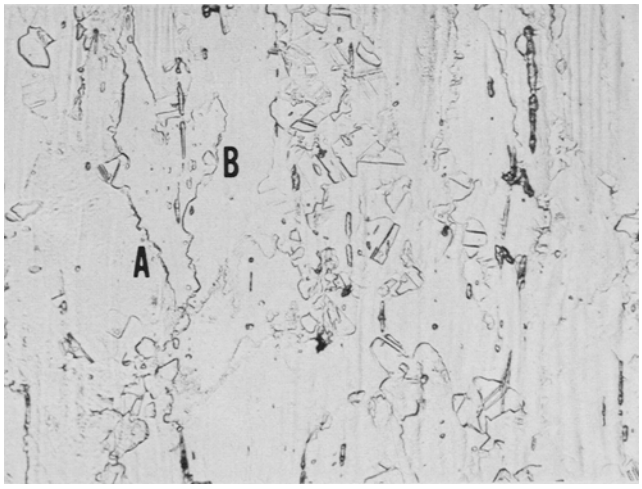

(*a*)

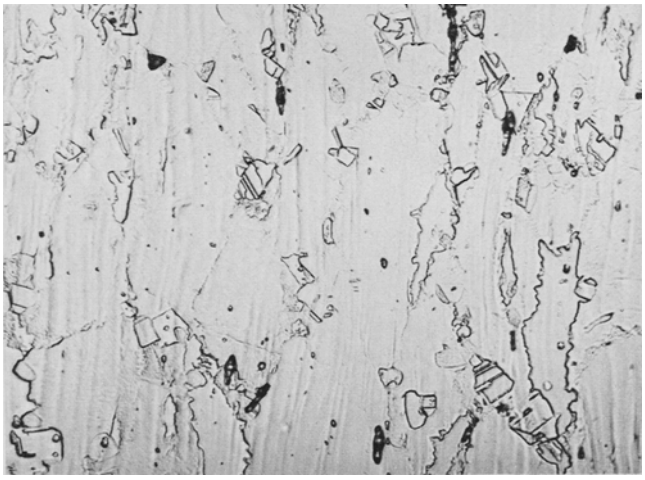

(*b*)

Fig. 11—Microstructure of 304 stainless steel deformed 50 pct at 1900°F. Magnification 423 times. (*a*) As deformed; (*b*) after a delay time of 0.038 s.

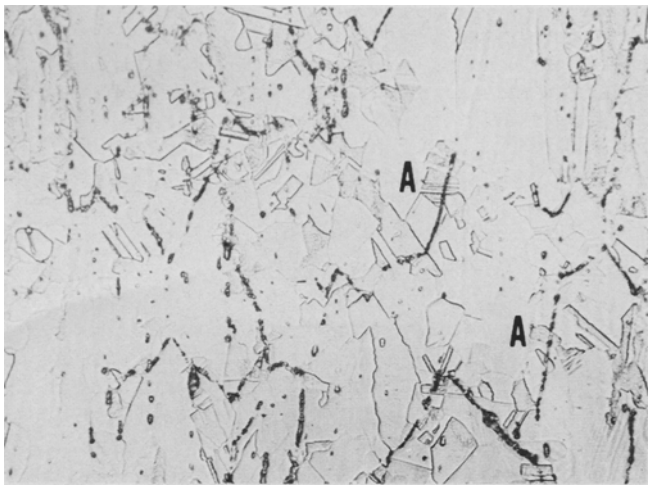

Fig. 12—Microstructure of 304 stainless steel partially recrystallized following 50 pct deformation at 1600°F. Magnification 423 times.

delay times for 50 pct deformation at 1750°F. The main features of importance are the rather clearly-defined microtwins within very elongated grains and the appearance of recrystallized grains which gradually consume the entire matrix. In general these changes in microstructure can be correlated very well with the load-softening data. The micrograph in Fig. 9 indicates the rather high density of the microtwins toward the end of the intermediate offset for 35 pct deformation at 1600°F. These micrographs lend support to the model of microtwin formation acting as a recovery mechanism in this material.

The micrographs in Fig. 10 indicate the appearance of the microstructure as deformed 50 pct at 1600°, 1750°, and 1900°F. The time between the end of deformation and the start of quenching was less than 0.001 s for the specimen deformed at 1900°F. Even with such a short delay time there is considerable evidence of recrystallization. The quench rate was approximately 500°F/s. It might be argued that the observed recrystallization took place during cooling to room temperature. The micrographs in Fig. 11 indicate, however, that no additional recrystallization takes place even for intentional short delay times after deformation. If the observed recrystallization took place during quenching, additional recrystallization would be expected with an intentional delay. The only change observable is a coarsening of the recrystallized grains. Thus, they must have formed during deformation. There is also a decrease in the extent of dynamic change with decreasing temperature and deformation. This lends support to the theory that dynamic recrystallization can indeed be an operating softening mechanism during deformation at high temperatures and large strains in low stacking-fault energy materials where recovery processes are inhibited. The micrograph in Fig. 11(*a*) also illustrates the high degree of boundary migration during deformation as evidenced by the ragged nature of the boundaries at point (*A*). It also shows what appears to be a recrystallization nucleus forming by boundary migration at point (*B*). Another interesting aspect of the recrystallization behavior is indicated in Fig. 12 which shows the preference for grain boundary nucleation. This micrograph corresponds to a partially-recrystallized specimen

during annealing at 1600°F. A peculiar aspect is the apparent outlining of the deformed grain boundaries due to a segregation effect which was not eliminated at this lower deformation temperature. It is fairly evident at point (*A*) that nucleation of recrystallized grains has taken place at the deformed boundaries.

CONCLUSIONS

In summary the major observations made in this investigation are:

1) As the temperature and/or the extent of deformation decreases, the rate of recrystallization following hot-working decreases. This is reflected in the apparent activation energy for softening increasing with decreasing deformation.

2) The data suggests that precipitation may take place during the recrystallization of the HSLA steel and inhibit the softening process. Recrystallization is not completed until the precipitate coarsens to a relatively ineffective morphology.

3) Softening curves and microstructural observations for hot-worked 304 stainless steel indicate the following:

a) Thermal microtwinning is an active recovery mechanism during annealing.

b) Dynamic recrystallization, occurring at least in part by boundary migration, is an operating softening mechanism during hot-working.

c) There is a preference for grain boundaries as nucleation sites for recrystallized grain.

ACKNOWLEDGMENTS

The authors gratefully acknowledge the financial and technical support of the Climax Molybdenum Company of Michigan for making this investigation possible.

REFERENCES

1. J. G. Byrne: *Recovery, Recrystallization, and Grain Growth,* pp. 13-92 and 110-65, MacMillan Series in Materials Science, New York, 1965.
2. W. C. Leslie, J. T. Michalak, and F. W. Aul: *Iron and Its Dilute Solid Solution,* pp. 119-212, John Wiley and Sons, New York, 1963.
3. S. J. Basinski and Z. S. Basinski: *Recrystallization, Grain Growth, and Textures,* pp. 1-44, Amer. Soc. Metals, Metals Park, 1966.
4. H. J. McQueen: *J. Metals,* 1968, vol. 20, no. 4, pp. 31-38.
5. H. P. Stuwe: *Iron Steel Inst. Publ. No.* 108, 1958, pp. 1-6.
6. J. J. Jonas, C. M. Sellars, and W. J. McG. Tegart: *Met. Rev.,* 1969, vol. 14, no. 130, p. 1.
7. D. J. Blickwede: *New Knowledge About Sheet Steels,* 1970, Amer. Soc. Metals, Metals Park, pp. 15-26.
8. James C. M. Li: *Recrystallization, Grain Growth and Textures,* pp. 45-97, Amer. Soc. Metals, Metals Park, 1966.
9. J. J. Jonas, H. J. McQueen, and W. A. Wong: *Iron Steel Inst Publ. No.* 108, 1968, pp. 49-59.
10. R. W. Cahn: *Proc. Royal Soc., London,* 1950, vol. A63, p. 323.
11. J. E. Burke and D. Turnbull: *Progr. Metal Phys.,* vol. 3, p. 220, Pergamon Press, New York, 1952.
12. R. W. Cahn: *Recrystallization, Grain Growth, and Textures,* pp. 99-128, Amer. Soc. Metals, Metals Park, 1966.
13. V. Ramaswamy and D. R. F. West: *J. Iron Steel Inst.,* 1970, vol. 208, pp. 395-400.
14. S. F. Reiter: *Trans. AIME,* 1952, vol. 194, p. 972.
15. R. E. Reed-Hill: *Physical Metallurgy Principles,* p. 175, D. Van Nostrand Co., Inc., Princeton, 1964.
16. T. Jormalainen and J. Pietikaine: *Acta Polytech. Scand.,* 1968, [CH], vol. 72, pp. 1-22.
17. C. S. Smith: *Trans. AIME,* 1948, vol. 175, p. 15.
18. E. C. W. Perryman: *Trans. AIME,* 1955, vol. 203, p. 369.
19. A. T. English and W. A. Backofen: *Trans. TMS-AIME,* 1964, vol. 230, pp. 396-407.
20. R. Priestner, C. C. Earley, and J. H. Randall: *J. Iron Steel Inst.,* 1968, vol. 206, pp 1252-62.
21. M. J. Luton and C. M. Sellars. *Acta Met.,* 1969, vol. 17, pp. 1033-43.
22. E. Shapiro and G. E. Dieter. *Met. Trans.,* 1970, vol. 1, pp. 1711-19.
23. W. J. McG. Tegart: *Ductility,* pp. 133-77, Amer. Soc. Metals, Metals Park, 1968.
24. W. C. Leslie, R. L. Rickett, C. L. Dotson, and C. S. Walton: *Trans. ASM,* 1954, vol. 46, pp. 1470-97.
25. R. L. Rickett and W. C. Leslie: *Trans ASM,* 1959, vol. 51, pp. 310-33.
26. J. T. Michalak and H. W. Paxton: *Trans. TMS-AIME,* 1961, vol. 221, pp. 850-57.
27. W. C. Leslie: *Trans. TMS-AIME,* 1961, vol. 221, pp. 752-57.
28. W. C. Leslie, J. T. Michalak, A. S. Keh, and R. J. Sober: *Trans. ASM,* 1965, vol. 58, pp. 672-86.
29. J. D. Baird and J M. Arrowsmith: *J. Iron Steel Inst.,* 1966, vol 204, pp. 240-47.
30. V. Ramaswamy, A. E. Summer, and D. R. F. West: *J. Iron Steel Inst.,* 1968, vol. 206, pp. 85-88.
31. H. Kubota and I. Kozasu: Technical Research Laboratory, Nippon Kohan K. K., Kawasaki, Japan, *TMS Paper No.* A68-53, 1968, pp. 1-21.
32. D. A. Witmer and R. M. Willison: *J. Metals,* 1970, vol. 22, no. 4, pp. 56-62.
33. K. Farrell, A. C. Schaffhauser, and J. T. Houston: *Met. Trans.,* 1970, vol. 1, pp. 2899-2905.
34. A. P. Gulyayev and A. S. Shigarev: *Fiz. Metal. Metalloved.,* 1964, vol. 18, pp. 233-38.
35. D. I. Bron, I. I. Levites, and M. N. Shashina: *Metalloved. Term. Obrab. Metal.,* 1965, no. 2, pp. 44-46.
36. R. S. Cremisio, H. M. Butler, and J. F. Radavich: *J. Metals,* 1969, vol. 21, no. 11, pp. 55-61.
37. G. A. Wilber, J. R. Bell, J. H. Bucher, and W. J. Childs: *Trans. TMS-AIME,* 1968, vol. 242, pp. 2305-08.
38. J. N. Cordea and R. E. Hook: *Met. Trans.,* 1970, vol. 1, pp. 111-18.
39. W. F. Savage: *J. Appl. Polym Sci.,* 1962, vol. 6, pp. 303-15.
40. A. Omsen and B. E. Skoog: *Metal Progr.,* 1970, vol. 97, no. 4, pp. 75-76.
41. W. J. Murphy and R. B. G. Yeo: *Metal. Progr.,* 1969, vol. 96, no. 3, pp. 85-89.
42. J. D. Jones and A. B. Rothwell. *Iron Steel Inst. Publ. No.* 108, 1968, pp. 78-82.